

INVESTIGATING GEOTHERMAL ENERGY RESOURCE POTENTIAL IN PARTS OF SOUTH WESTERN NIGERIA USING AEROMAGNETIC DATA

Mamman Grace Ayuba*¹ and M. K. Lawal²

Department of Physics, Ahmadu Bello University, Zaria

Authors' Email Addresses: grace2ayuba1@gmail.com*¹ and kola2lawal@yahoo.com

ABSTRACT

The investigation of geothermal energy resources potential in this study involves delineating targets areas of the earth's crust where geologic processes have raised temperatures near the surface, such that the heat contained can be utilised. A high-resolution aeromagnetic (HRAM) data of part of south-western Nigeria on longitude 3.5° to 5.5° and latitude 7.0° to 9.0° consisting of 16 half degree sheet was used for this research work. Spectral analysis was applied in processing HRAM data, which transforms the spatial data into the frequency domain, and provides a relationship between the two-dimensional spectrum of the magnetic anomalies. Results indicates that the average Curie point depth (CPD) within the study area is 8.5 km followed by the average geothermal gradient of 42.5°Ckm⁻¹ and an average heat flow 55 mWm⁻². The equitable promising geological results useful for geothermal exploitation is within longitude 4.2° to 4.6° and latitude 7.8° to 8.2°, where the lowest CPD (5.5km), highest geothermal gradient (75°Ckm⁻¹) and highest heat flow (190mWm⁻²) bounded by Oshogbo and Ogbomosho as indicated on the maps. The paper suggests that such an area can be considered for geothermal energy exploitation since the demagnetized of magnetic rocks confirms a hot rock who's temperature of about 580°C.

Keywords: Geothermal energy, resource potential, Curie temperature, geothermal gradient, heat flow.

INTRODUCTION

The West African Rift System led to the formation of the Benue Trough in Nigeria, creating sub-basins within the Trough (Abraham & Itumoh, 2019). These basins were subjected to synsedimentary tectonic deformations during Cretaceous to Neogene times and were affected by magmatic—volcanic episodes leading to multiple areas of geothermal anomalies within sedimentary basins that also affected the entire south western Nigeria.

Geothermal energy resource differs from any other renewable energy resource, so it has an edge over other renewables. Geothermal energy is the energy contained in the intense heat of the earth that continually flows outward from deep inside the earth. It can be accessed and exploited by drilling hot water or steam as the case may be in a process similar to drilling of oil and natural gas. Geothermal energy when compared with other renewables is an enormous, underuse heat and power resource that emits little or no greenhouse gasses (Dipippo & Renner, 2014). The search for geothermal resources focuses on those areas of the earth's crust where geologic processes have raised temperatures near the surface such that the heat contained can be utilised. Such areas are seen to include; Fractured and thinned crust which allow the

magma to rise to the surface as lava that comes because of the volcanic events within the earth (Whitmarsh, 2001). Even though the greatest part of the heat that accompanied the lava within the earth does not get to the surface, but heats up the underlying rocks. As rainwater flows down through the fissure fracture and joints, this water gets heated up by the underlying rocks. The pressure within the earth forces the hot water out to the surface as steam, source of warm spring, fumaroles and the like. When these sources are harnessed and trap in a permeable rock under an impermeable rock it will form a geothermal reservoir that will later serve as a source of geothermal energy. The mantle plume is an upwelling of abnormally hot rock within the earth's mantle. As the head of the mantle plumes can partly melt when they reach shallow depths, they are thought to be the cause of volcanic centres known as hot spots and probably caused the flood of basalts.

The geothermal energy has its origin in proximity to the Mantle plume, thermal uplift, pressure from sediments, radioactive decay (radiogenic) of various minerals inside the Earth's core and the residual heat produced in the planet's formation millions of years ago (Nemzer, 2009; GEA, 2012; Ned, 2012; Richter, 2017). Wohletz & Heiken (1992) express that geothermal energy is an important and promising alternative energy resource that has shown continual growth throughout this century. Among the renewables, geothermal energy can produce year-round constant power, a significant differentiation from both solar and wind power, which must wait for the sun to shine or the wind to blow, respectively.

According to (DiPippo & Renner, 2014; Hamilton, 2014; Letcher, 2013), geothermal energy has the following advantages over other sources of renewable energy: It is one of the cleanest forms of energy now available in commercial quantities.

- It avoids the problems of acid rain and greatly reduces greenhouse gas emissions and other forms of air pollution.
- Potentially hazardous elements produced in geothermal brines are usually injected back into the producing reservoir.
- Land use for geothermal wells, pipelines and power plants is small compared to land use for other extractive energy sources such as oil, gas, coal and nuclear.
- Geothermal development projects often coexist with agricultural land uses including crop production or grazing.
- The low life-cycle land use of geothermal energy is many times less than the energy sources based on mining, such as coal and nuclear, that require enormous areas for mining and processing before fuel reaches the power plant.
- Hydroelectric projects with massive dams inundate and occupy vastly more land than any type of geothermal plant per installed megawatt.

- Low-temperature applications usually are no more intrusive than water well.
- Geothermal development serves the growing need for energy sources with low atmospheric emissions.
- In most geothermal systems, NCGs make up less than 5 % by weight of the steam phase. For example, for each megawatt-hour of geothermal electricity produced in flash steam plants in the United States, the average emission of CO₂ is only about 5 % of that emitted when natural gas is burned in a combustion turbine to produce electricity.

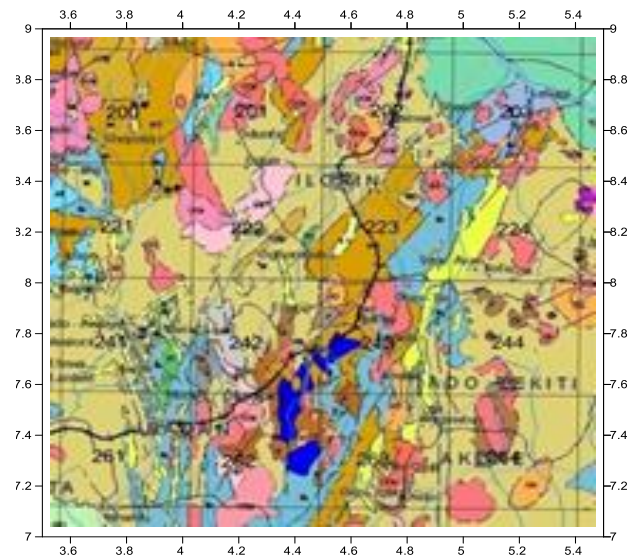
Because of how significant these advantages are it's important to investigate the geothermal resource potential of the study area.

Geology of the Area of Study

The study area occupies parts of South-Western Nigeria covering 16 standards 1:100,000 topographic sheets as shown in Figure 1 Major geologic components of the area include the Basement Complex Rocks and parts of the Sedimentary Basins of the Bida basin.

A. Basement Complex

The Nigerian basement complex forms a part of the Pan-African mobile belt and lies between the West African and Congo Cratons and south of the Tuareg Shield (Black, 1980). The basement complex was affected by the 600 Ma Pan-African orogeny and occupies the reactivated region which resulted from plate collision between the passive continental margin of the West African craton and the active Pharusian continental margin (Burke & Dewey, 1972; Dada, 2006). The basement rocks are believed to be the results of at least four major orogenic cycles of deformation, metamorphism and remobilization corresponding to the Liberian (2,700 Ma), the Eburnean (2,000 Ma), the Kibaran (1,100 Ma), and the Pan-African cycles (600 Ma). The first three cycles were characterized by intense deformation and isoclinal folding accompanied by regional metamorphism, which was further followed by extensive migmatization. The Pan-African deformation was accompanied by a regional metamorphism, migmatization, extensive granitization and gneissification which produced syntectonic granites and homogeneous gneisses (Abaa, 1985). Late tectonic emplacement of granites and granodiorites and associated contact metamorphism accompanied the end stages of this last deformation. The end of the orogeny was marked by faulting and fracturing (Gandu *et al.*, 1986; Olayinka, 1992).



Explanation

SDP	Sand, Clay and Swamp
Css	Sands, Clays, siltstones and limestones
CPs	Sand and Clay
bb	Babai
Lsr	Lignite, Claystone and shale
lsh	Clay clayey sands and shale
Gss	Sandstone and Clay
UCM	Sandstone, Limestone, Coal
Asl	Sandstone and Limestone
Mst	Coal, Sandstone and Shale
OGb	Coarse Porphyritic hornblende granite
OGc	Porphyritic Granite
OGf	Fine-grained biotite granite
OGm	Medium-to coarse-Grained Biotite granite
OGu	Undifferentiated granite, Migmatite
Ch	Charnockitic Rocks
bG-b	Biotite Hornblende Gneiss
bS	Biotite Garnet Gneiss Schist
OPg	Porphyroblastic Gneiss
GG	Granite Gneiss
Ge	Quartz feldspathic granulite and gneiss
BO	Banded Gneiss / Biotite Gneiss
MeG	Migmatitic augen Gneiss
MO	Migmatitic Gneiss
M	Migmatite

Figure 1: Geological Map of the Study Area

Geothermal energy investigations

Nwankwo *et al.* (2011), investigate heat flow anomalies in Nupe Basin, results showed that geothermal gradient varies between 10 °C/km and 45 °C/km while ensuing heat flow varies between 20 mW/m² and 120 mW/m² in the SE and SW of their study area. Megwara *et al.* (2013), also studies on parts of Southern Bida Basin of Nigeria and the surrounding basement rocks used aeromagnetic data and radioactive sources to obtain heat flow

values of range 69.167 mWm^{-2} to 124.821 mWm^{-2} with an average value of 90.959 mWm^{-2} . Heat flow were found to be less than 60 mWm^{-2} while flow more than 100 mWm^{-2} are found in NE, NW parts, based on the submission of Obande *et al.* (2014), that average heat flow in thermally normal continental regions is reputed to be above 60 mWm^{-2} , values more than 80 mWm^{-2} to 100 mWm^{-2} , indicate anomalous geothermal conditions. They observed anomalies of above 100 mWm^{-2} and hence called for further investigation. While Nwankwo & Sunday (2017), estimated the Curie point depths, geothermal gradient and subsurface crustal heat flow regionally, using aeromagnetic data of Bida Basin on latitude 8.00°N to 10.50°N and longitude 4.50°E to 7.50°E . Results show that CPD varies between 15.57 and 29.62 Km and the geothermal gradient varies between $19.58 \text{ }^\circ\text{CKm}^{-1}$ and $37.25 \text{ }^\circ\text{CKm}^{-1}$ while the heat flow varies from 48.41 and 93.12 mWm^{-2} . Thus, areas with low CPDs and corresponding high heat flow in their study area suggested anomalous geothermal conditions. The world heat data collection in 1975 from Geological Survey of Canada by Jessop *et al.*, (1976) shows that values of heat flow well above 100 mWm^{-2} are above the normal thermally continental areas, which imply that there is an anomalous heat flow

MATERIALS AND METHOD

The study area is covered by a High Resolution Aeromagnetic (HRAM) data. The survey was conducted by the Nigeria Geological Survey agency in the year 2005 to 2010 and HRAM data were obtained using a proton precession magnetometer with a resolution of 0.01 nT . Fugro Airborne Surveys carried out the airborne geophysical work. The Aeromagnetic surveys were flown at a line spacing of 500 m and at terrain clearance of 80 m , at a map scale of $1:100,000$ series. Each sheet has an area of 55 km by 55 km giving a total area of 45375 km^2 . A total of fifteen (15) sheets were purchased from the Nigeria Geological Survey Agency (NGSA). These include sheets 200 - 203, 221 - 224, 241 - 244 and 261 - 264 covering the entire study area. The total intensity aeromagnetic data for the study area compiled by the Nigeria Geological Survey Agency (NGSA) is shown in Figure 2.

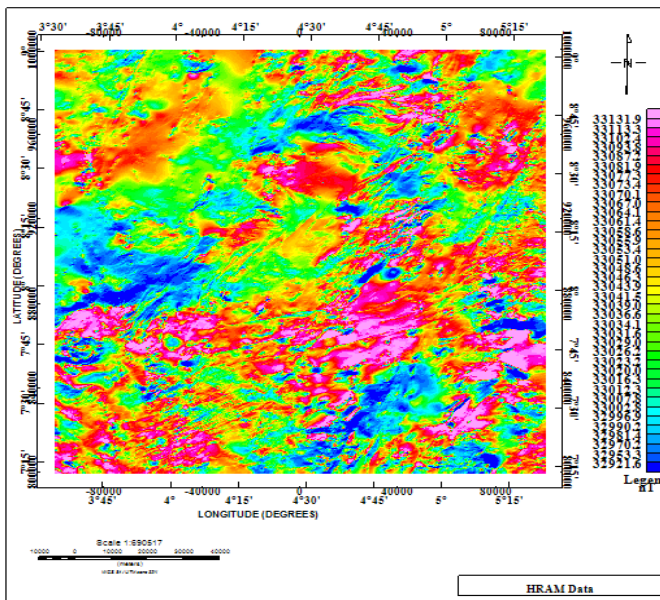


Figure 2: The HRAM Map

The HRAM data Figure 2 are useful for geothermal resource potential mapping at a variety of scales (Abu El -Ata *et al.*, 2013). It is used for the estimation of CPD, Heat Flow and Thermal Gradient. To estimate the Curie point (basal) depth Z_b of the magnetic source, Tanaka *et al.* (1999) assumed that the layer of the magnetic source extends infinitely in all horizontal directions, and that the depth to a magnetic source's horizontal scale, and the magnetization $M(x,y)$ is a random function of x and y . Blakely (1995) showed that the power density spectra of the total field anomaly P is given by

$$P(k_x, k_y) = P(k_x, k_y) \times F(k_x, k_y)$$

$$F(k_x, k_y) = 4\pi^2 C_m^2 |\theta_m|^2 |\theta_f|^2 e^{-2|k|Z_t} [1 - e^{-|k|(Z_b - Z_t)}]^2 \quad (1)$$

Where P , is the power density spectrum of the Magnetization, C_m is proportionality constant, θ_m and θ_f are factors for magnetization and geomagnetic field direction respectively. Z_b and Z_t are depths to bottom and top of the magnetic source respectively. The equation can be simplified by noting that all terms except $|\theta_m|^2$ and $|\theta_f|^2$ are radially symmetric. Furthermore, the radial averages of θ_m and θ_f are constants. If $P(x,y)$ is completely random and uncorrelated, $P(k_x, k_y)$ is a constant. Hence, the radial average of P is:

$$P(|k|) = A e^{-2|k|Z_t} [1 - e^{-|k|(Z_o - Z_t)}]^2 \quad (2)$$

Where A is a constant and k is the wave number. For wavelengths less than about twice the thickness of the layer Equation (2) can be written as equation (3)

$$\ln P |k|^{\frac{1}{2}} = \ln B - |k|Z_t \quad (3)$$

Where B is a constant. The upper bound of magnetic source Z_t could be estimated by fitting a straight line through the high-wave number part of a radially average power spectrum $[\ln P |k|^{\frac{1}{2}}]$.

$$P(|k|)^{\frac{1}{2}} = C e^{-|k|Z_o} (e^{-|k|Z_t - Z_o} - e^{-|k|Z_b - Z_o}) \quad (4)$$

Where C is a constant, a long wavelength, equation (4) can be rewritten as

$$P(|k|)^{\frac{1}{2}} = C e^{-|k|Z_o} (e^{-|k|(-s)} - e^{-|k|(s)}) \approx C e^{-|k|Z_o} 2|k|s \quad (5)$$

Where $2s$ is the thickness of the magnetic source. From equation (5), it can be concluded that

$$\ln \left\{ \frac{P |k|^{\frac{1}{2}}}{|k|} \right\} = \ln D - |k|Z_o \quad (6)$$

Where D is a constant. The centroid of the magnetic source Z_o can be estimated by fitting a straight line through the lower-wave number part of the radially average frequency scale power spectrum average power

Then the Basal Depth Z_b of the magnetic source will be calculated

from the equation

$$Z_b = 2Z_o - Z_t \quad (7)$$

Z_o is the centroid of the magnetic source Z_t is the depth to the top of the magnetic source, while Z_b is the basal depth of the magnetic sources assumed to be the Curie point depth (Bhattacharyya and Lue, 1975; Okubo *et al.*, 1985). At the basal depth Z_b Ferromagnetic minerals are converted to Paramagnetic minerals due to a temperature of approximately 580°C (853 K) at that depth.

The basic relation for conductive heat transport is the Fourier's law. Tanaka *et al.* (1999) showed that any given depth of a thermal isotherm is inversely proportional to the heat flow. In a one-dimensional case under assumptions, the direction of the temperature variation is vertical and the temperature gradient $\frac{dT}{dz}$ is constant, Fourier's law takes the form

$$q = k \frac{dT}{dz} \quad (8)$$

q is the heat flux measured in units of energy, the SI unit being W/m^2 . k is the coefficient of thermal conductivity which is a measure of how easily heat flows through a material, the SI unit for k is $Wm^{-1}K^{-1}$ or $Wm^{-1}C^{-1}$. $\frac{dT}{dz}$ is the temperature gradient. The thermal gradient is being calculated as follows

$$\frac{dT}{dZ} = \frac{T_c - T_s}{Z_b} = \frac{580^\circ C - T_s}{Z_b} \quad (9)$$

Where T_s the surface temperature.

The surface temperatures used in this work was extracted from the map of surface temperature study of Shchoneich, (1998).

The Heat Flow values are calculated using equation (10)

$$q = k \left(\frac{dT}{dZ} \right) = k \frac{580^\circ C - T_s}{Z_b} \quad (10)$$

Where q is the heat flow and k the coefficient of thermal conductivity. The k value differs within the study area; the variation in this value is as result of the different rock units that are within the study area.

RESULTS AND DISCUSSION

The first result obtained are those of the spectral plot shown in figure 3 (a), just a sample because all the results for depth to top (Z_t) and depth to centroid (Z_o) obtained from the plots have been extracted and presented on tables 1 and 2 respectively. Followed by the results for depth to bottom, geothermal gradient (GTG) and Heat flow (HF) obtain from the use of equations 7, 8 and 9 respectively also presented on table 1 and 2 respectively.

The results presented on table 1 and 2 were harnessed and used to processed the maps of depth to top, depth to centroid, depth to bottom, geothermal gradient and heat flow shown in figure 3 (b) to (f) respectively.

The **depth to Top Map** figure 3 (b) shows a variation in the depth to top of the magnetic anomaly to be shallower at some points represented in blue to purple and deepest at other points represented in orange. The depth to top of the magnetic anomalous hot bodies indicates accessible depths to geothermal energy

resource potential. The average value for the entire study area is 0.95 km, with a range of 0.5 km to 1.45 km. At depths of 0.5 km, drilling will be easier than at depths of 1.45 km which implies that accessibility of geothermal resource is cost effective at shallower depths and capital intensive at greater depths considering the cost of drilling. The area bounded by towns like; Ibadan, Oshogbo, Ogbomoso and Ilorin fall within the least depth to top values which are between 0.5 km to 0.7 km.

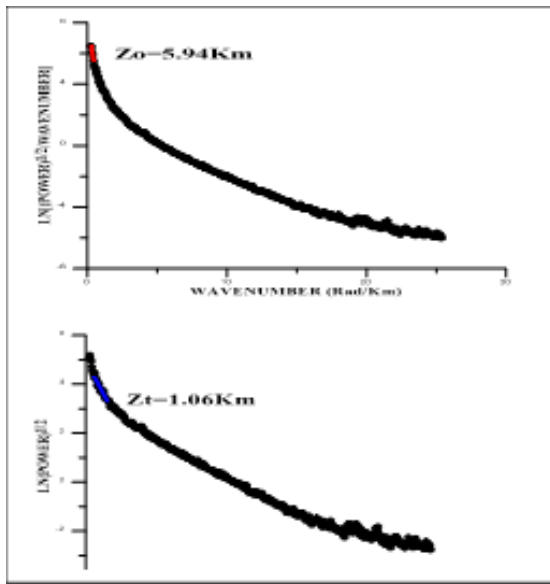
The **Depth to Centroid Map**, Figure 3 (c) of the study area also showed varying depth with an average of 5.5 km, with 3 km as the least and 8.0 km as the highest values. The highest depth to centroid is found to dominate mid-south at depth 8.0 km, to south-eastern part bounded by Ekiti at depth of 7.4 km of the study area as indicated by the contour lines on the map. While the least dominates the middle of the study area bounded by Oshogbo and Ogbomoso at longitude $4.2^\circ E$ to $4.8^\circ E$ and Latitude $7.8^\circ N$ to $8.2^\circ N$ at depth of 3.0 km which is at the mid-point of the study area. Followed by an area around Ibadan at longitude $3.6^\circ E$ to $4.0^\circ E$ and latitude $7.2^\circ N$ to $7.8^\circ N$ at a depth of 4.0 km south western part of the study area. The highest depth to centroid 8.0 km is within longitude $4.2^\circ E$ to $4.8^\circ E$ and latitude $7.2^\circ N$ to $7.8^\circ N$ mid-south of the study area with an area of depth to centroid 5.4 km south-west towards the extreme end of the study area.

Table 1: Results for the Single Block window

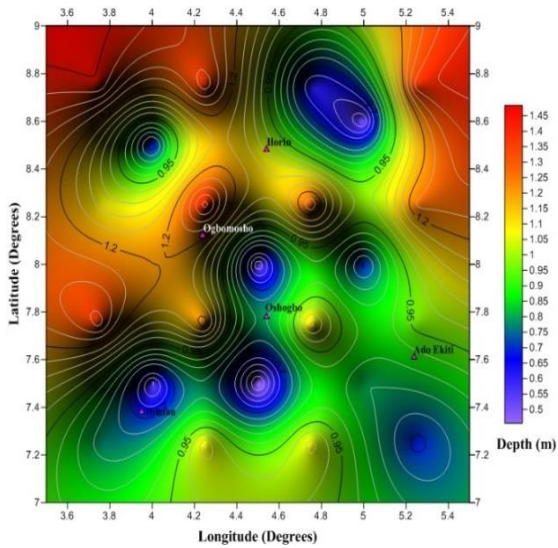
Block	Longitude (Degrees)	Latitude (Degrees)	C	Z_t (km)	Z_b (km)	GTG $^\circ C km^{-1}$	HF $mW m^{-2}$
200	3.75	8.75	6.66	1.44	11.89	16.55172	49.65517
201	4.25	8.75	6.99	1.38	12.6	13.92857	41.78571
202	4.75	8.75	5.08	0.6	8.96	31.77455	95.32366
203	5.25	8.75	6.9	1.38	12.41	14.60113	36.50282
221	3.75	8.25	5.85	1.09	10.62	22.11864	55.29661
222	4.25	8.25	4.93	1.43	8.44	35.58057	88.95142
223	4.75	8.25	5.63	1.3	9.96	25.57229	51.14458
224	5.25	8.25	6.02	1.26	10.79	21.2975	53.24374
241	3.75	7.75	4.72	1.37	8.06	38.61042	77.22084
242	4.25	7.75	7.62	1.23	14.01	9.471806	23.67951
243	4.75	7.75	6.01	1.12	10.9	20.73394	62.20183
244	5.25	7.75	7.48	0.97	13.98	9.556509	14.33476
261	3.75	7.25	4.92	0.78	9.06	31.12583	62.25166
262	4.25	7.25	6.76	1.08	12.44	14.45338	36.13344
263	4.75	7.25	6.76	1.07	12.45	14.41767	36.04418
264	5.25	7.25	5.75	0.68	10.81	21.15634	52.89084

Table 2: Results for the Optimized Block Window

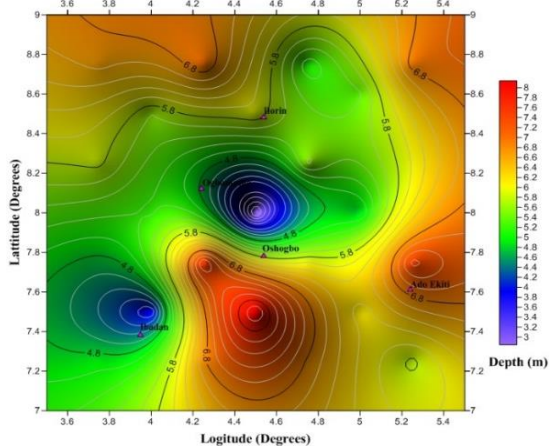
Block	Longitude (Degrees)	Latitude (Degrees)	z_o (m)	z_t (km)	z_b (km)	GTG $^\circ C km^{-1}$	HF $mW m^{-2}$
11	4	8.5	5.6	0.65	10.55	22.46445	56.16114
12	4.5	8.5	5.94	1.06	10.82	21.15527	52.88817
13	5	8.6	5.37	0.5	10.24	24.05273	60.13184
19	4	8	5.18	1.2	9.16	30.42576	76.06441
20	4.5	8	2.72	0.5	4.94	82.04453	205.1113
21	5	8	4.79	0.68	8.9	32.13483	80.33708
27	4	7.5	3.82	0.53	7.11	47.77778	119.44444
28	4.5	7.5	8.2	0.43	15.97	4.627426	11.56857
29	5	7.5	6.12	0.8	11.44	18.33916	55.01748



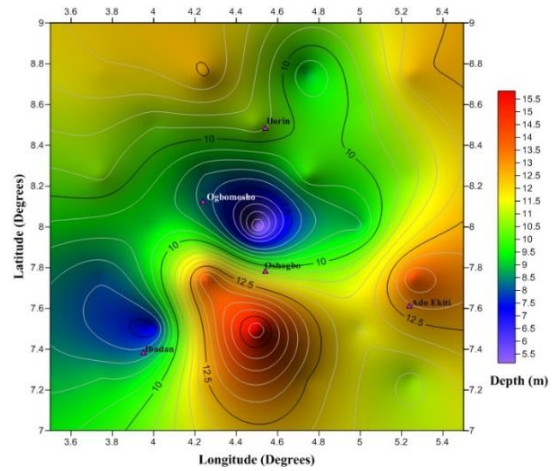
(a): A sample of the spectral Plot



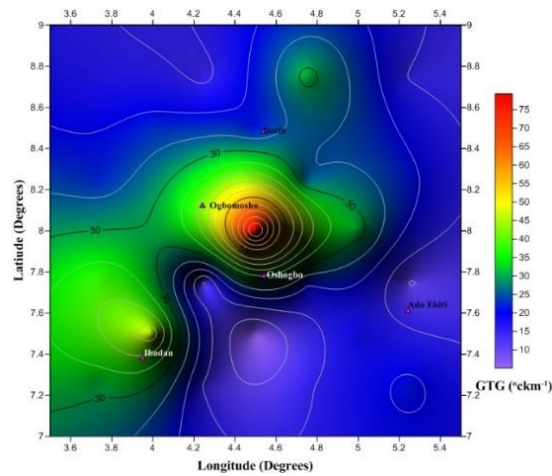
(b) Map of Depth to Top



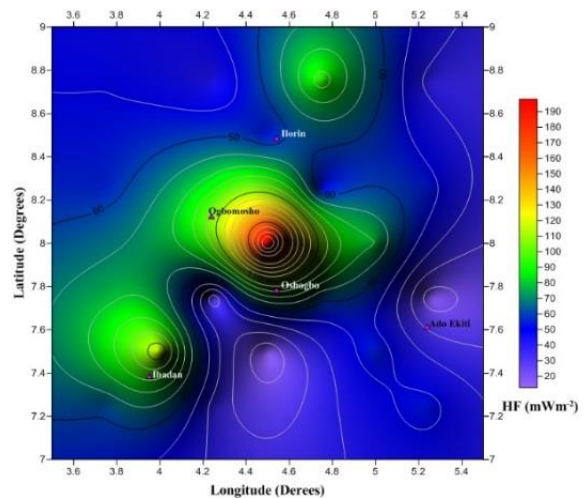
(c): Map of Depth to Centroid



(d): Map of Depth to Bottom



(e): Map of Geothermal Gradient



(f): Map of Heat Flow

Figure 3: Results of Spectral Plots (a), Depth to Top map (b), depth to Centroid map (c) Curie point depth map (d), geothermal Gradient (e) map and Heat Flow map (f)

The **Curie Point Depth (CPD) Map** figure 2 (d) indicate the depth at which the magnetic anomaly loses its magnetism at Curie temperature (T_c). The average depth in the study area is 10.5 km with 5.5 km and 15.5 km as the lowest and highest values respectively. The highest CPD is found to dominate south at depth 15.5 km, to south-eastern part at depth of 13.3 km of the study area as indicated by the map. While the least dominates the middle of the study area bounded by Oshogbo and Ogbomosho at longitude $4.2^{\circ}E$ to $4.8^{\circ}E$ and Latitude $7.8^{\circ}N$ to $8.2^{\circ}N$ at depth of 5.5 km which is almost at the mid-point of the study area. Followed by an area around Ibadan at longitude $3.6^{\circ}E$ to $4.0^{\circ}E$ and latitude $7.2^{\circ}N$ to $7.8^{\circ}N$ at a depth of 7.5 km south western part of the study area. Results of CPD obtained in this research agrees with the CPD values obtained by (Abraham *et al.*, 2014), obtain at Ikogosi warm spring.

The **Geothermal Gradient Map (Figure, 3e)** ; indicate that the geothermal gradient in ($^{\circ}Ckm^{-1}$) show the rate of depth dependent temperature growth. Figure 3 (e) showed this depth dependent temperature growth range $10^{\circ}Ckm^{-1}$ to $75^{\circ}Ckm^{-1}$ with an average value of $42.5^{\circ}Ckm^{-1}$. The high geothermal gradient values fall within latitude $7.8^{\circ}N$ to $8.2^{\circ}N$ and longitude $4.2^{\circ}E$ to $4.8^{\circ}E$, bounded by Oshogbo and Ogbomosho. The lowest values are found to be in the mid-south with $10^{\circ}Ckm^{-1}$ NW, NE and SE $25^{\circ}Ckm^{-1}$ parts of the study area. It is interesting to note that the values of the geothermal gradient shown in the NE and SE parts of this study agrees with those of the previous researchers (Nwankwo *et al.* 2011; Megwara *et al.* 2013; Nwankwo & Sunday, 2017) in parts of the study area.

The **Heat Flow** values are divided into three major sections as indicated on the map Figure 3(f). The low values are of range $20 mWm^{-2}$ to $60 mWm^{-2}$ which is below the range of the normal continental fields. Then the intermediate heat flow with values of $60 mWm^{-2}$ to $110 mWm^{-2}$ fall within the rage of heat flow values in the normal geothermal continental fields. Also, the intermediate crustal heat flow values agree with those of (Nwankwo & Sunday, 2017) that worked in parts of Bida basin which is part of the present study. While the range of the maximum ($110 mWm^{-2}$ to $190 mWm^{-2}$) is above the range for the normal continental fields, which can be said to be anomalous heat flow. This is an indication that the heat flow could be sufficient if extracted to serve as an additional energy source. The area with the high flow is within the same location with that of the geothermal energy.

Conclusion

The study shows areas with prospects for geothermal energy resource potential to be where the geothermal gradient is high ($45^{\circ}Ckm^{-1}$ to $75^{\circ}Ckm^{-1}$) and high heat flow ($110 mWm^{-2}$ to $190 mWm^{-2}$) have high prospects for geothermal energy. These areas are Oshogbo and Ogbomosho located within latitude $7.8^{\circ}N$ to $8.2^{\circ}N$ and Longitude $4.2^{\circ}E$ to $4.6^{\circ}E$.

The geothermal energy resource potential result obtained in this research, if exploited can serve as an alternative source of energy that will reduce the effects global warming posed by fossil fuel and other non-renewable energy resources.

Recommendation

The results of this research recommends that drilling being the most accurate technique that can give the accurate result should be carried out by the government agency concerned in the in the protective zones identified after applying others like magnetotellurics which allows detection of resistivity anomalies associated with productive geothermal depths to ascertain the result obtained in this research. So that if exploited can serve as an alternative source of energy that will reduce the effects global warming created by fossil fuel.

Contribution to knowledge: Results obtained in this research work forms a basis for further investigation of geothermal energy potential in the study area.

Acknowledgment

We thank Nigerian Geological Survey Agency for the provision of the High Resolution Aeromagnetic (HRAM) Data.

REFERENCES

- Abaa, S. I. (1985). The structure and petrography of alkaline rocks of the Mada Younger Granite complex, Nigeria. *Journal of African Earth Sciences* (1983), 3(1), 107-113.
- Abraham, E. M., and Itumoh, O. E. (2019). Geothermal Reconnaissance of Southeastern Nigeria from Analysis of Aeromagnetic Data. In *On Significant Applications of Geophysical Methods* (pp. 43-46). Springer, Cham.
- Abraham, E. M., Lawal, K. M., Ekwe, A. C., Alile, O., Murana, K. A., and Lawal, A. A. (2014). Spectral analysis of aeromagnetic data for geothermal energy investigation of Ikogosi Warm Spring-Ekiti State, southwestern Nigeria. *Geothermal Energy*, 2(1), 1.
- Abu El-Ata A.S, Al-Khateef A.A., Ghoneimi A.E, Abd Alnabi S.H and Al-Badani M.A (2013). Applications of Geomagnetic data to detect basement tectonics of Eastern Yemen. *Egyptian journal of petroleum volume 22, issue 2, December 2013, pp 277-292*
- Bhattacharyya, B. K., and Leu, L. K. (1975). Analysis of magnetic anomalies over Yellowstone National Park: Mapping of Curie point isothermal surface for geothermal reconnaissance. *Journal of Geophysical Research*, 80(32), 4461-4465.
- Black R., (1980) Precambrian of West Africa. Episodes 4:3-8
- Blakely, R.J., 1995. Potential Theory in Gravity and Magnetic Applications. Cambridge
- Burke K.C., Dewey J. F., (1972) Orogeny in Africa. In: Dessauvage TFJ, Whiteman AJ (eds), Africa geology. University of Ibadan Press, Ibadan, pp 583-608 Complex, Nigeria. *J Afr Earth Sci* 3:107-113.
- Dada S.S., (2006) Proterozoic Evolution of Nigeria. In: Oshi O (ed) The basement complex of Nigeria and its Mineral Resources (A Tribute to Prof. M. A. O. Rahaman). Akin Jinad and Co. Ibadan, pp 29-44
- Dippio, R., & Renner, J. L. (2014). Geothermal energy. In *Future Energy* (pp. 471-492).
- Encarta Dictionaries, (2009). By Microsoft Encarta.
- Gandu A. H., Ojo S. B., Ajakaiye DE (1986) A gravity study of the Precambrian rocks in the Malumfashi area of Kaduna State, Nigeria. *Tectonophysics* 126:181-194
- GEA, (2012) Geothermal basic Questions and answers. <http://geothermal.org/what.html.pp8>
- Hamilton, M. S. (2014). *Energy Policy Analysis: A Conceptual Framework: A Conceptual Framework*. Routledge.

- Jessop, A. M., Hobart, M. A., and Sclater, J. G., (1976). The World Heat Flow Data Collection 1975, Geothermal Services of Canada. *Geothermal Service* 50, 55–77.
- Letcher, T. M. (Ed.). (2013). *Future energy: improved, sustainable and clean options for our planet*. Elsevier.
- Megwara, J. U., Udensi, E. E., Olasehinde, P. I., Daniyan, M. A., and Lawal, K. M. (2013). Geothermal and radioactive heat studies of parts of southern Bida basin, Nigeria and the surrounding basement rocks. *International Journal of Basic and Applied Sciences*, 2(1), 125.
- Ned, Haluzan (2012) Geothermal Energy. [http://Earthheat.blogspot.com.ngenergy/search/label/Geothermal energy](http://Earthheat.blogspot.com.ngenergy/search/label/Geothermal%20energy).
- Nemzer, M. L., Carter, A. K and Nemzer, K. P., (2009): Geothermal Energy." Microsoft® Encarta® 2009 [DVD]. Redmond, WA: Microsoft Corporation, 2008.
- Nwankwo, L.I., Olasehinde, P.I., Akoshile, C.O., 2011. Heat Flow Anomalies from the Spectral Analysis of Airborne Magnetic Data of Nupe Basin, Nigeria. *Asian J. Earth Sci.*, 1(1), 1-6.
- Nwankwo, L. I., and Sunday, A. J. (2017). Regional Estimation of Curie-point Depths and Succeeding geothermal parameters from recently acquired high-resolution aeromagnetic data of the entire Bida Basin, north-central Nigeria. *Geothermal Energy Science*, 5(1), 1.
- Obande, G. E., Lawal, K. M., and Ahmed, L. A. (2014). Spectral Analysis of Aeromagnetic Data for Geothermal Investigation of Wikki Warm Spring, North-East Nigeria. *Geothermics*, 50, 85-90.
- Okubo, Y., Graf, R. J., Hansen, R. O., Ogawa, K., and Tsu, H. (1985). Curie point depths of the island of Kyushu and surrounding areas. Japan. *Geophysics*, 50(3), 481-494.
- Olayinka A. I. (1992) Geophysical siting of boreholes in crystalline basement areas of Africa. *Journal Afr Earth Sci* 14:197–207.
- Schoniech, (1998) Map of Annual Average Ground Surface (Stevenson Screen) Temperature Map Lecture
- Tanaka, A., Okubo, Y., & Matsubayashi, O. (1999). Curie point depth based on spectrum analysis of the magnetic anomaly data in East and Southeast Asia. *Tectonophysics*, 306(3-4), 461-470. Univ. Press, pp. 307–308.
- Whitmarsh, R. B., Manatschal, G., and Minshull, T. A. (2001). Evolution of magma-poor continental margins from rifting to seafloor spreading. *Nature*, 413(6852), 150.
- Wohletz, K., and Heiken, G. (1992). *Volcanology and geothermal energy* (p. 432). Berkeley: University of California Press.

Bio Data

Mamman Grace Ayuba is a doctoral student of the Department of Physics, Ahmadu Bello University Zaria, Nigeria. She has to her credit scholarly articles in both local and international journals of great repute. Mamman is a lecturer with the Kaduna State College of Education Gidan- Waya, Nigeria. Her research interests are in Geothermal Energy, etc

Prof. Kola M. Lawal is a Professor of Geophysics in the Department of Physics, Ahmadu Bello University Zaria Nigeria. He has to his credit scholarly articles in both local and international journals of great repute. He has graduated a good number of both masters and doctoral students.